Inorganic Chemistry

Article

pubs.acs.org/IC

Novel Cu(I)-Selective Chelators Based on a Bis(phosphorothioyl)amide Scaffold

Aviran Amir,[†,§] Alon Ezra,[†,§] Linda J. W. Shimon,[‡] and Bilha Fischer*[,†]

[†]Department of Chemistry, Bar Ilan University, Ramat-Gan 52900, Israel

[‡]Department of Chemical Research Support, The Weizmann Institute of Science, Rehovot 76100, Israel

Supporting Information

ABSTRACT: Bis(dialkyl/aryl-phosphorothioyl)amide (BPA) derivatives are versatile ligands known by their high metal-ion affinity and selectivity. Here, we synthesized related chelators based on bis(1,3,2-dithia/dioxaphospholane-2-sulfide)amide (BTPA/BOPA) scaffolds targeting the chelation of soft metal ions. Crystal structures of BTPA compounds **6** ($N^-R_3NH^+$) and **8** (NEt) revealed a *gauche* geometry, while BOPA compound **7** ($N^-R_3NH^+$) exhibited an *anti*-geometry. Solid-state ^{31}P magic-angle spinning NMR spectra of BTPA **6**-Hg(II) and **6**-Zn(II) complexes imply a square planar or tetrahedral geometry of the former and a distorted tetrahedral geometry of the latter, while both BTPA **6**-Ni(II) and BOPA **7**-Ni(II) complexes possibly form a polymeric structure. In Cu(I)-H_2O_2 system (Fenton reaction conditions) BTPA compounds **6**, **8**, and **10** (NCH_2Ph) were identified as most potent antioxidants (IC_{50} 32, 56, and 29 μM, respectively), whereas BOPA analogues **7**, **9** (NEt), and **11** (NCH_2Ph) were found to be poor antioxidants. In Fe(II)-H_2O_2 system, IC_{50} values for both BTPA and BOPA compounds exceeded 500 μM indicating high selectivity to Cu(I) versus the borderline Fe(II)-ion. Neither BTPA nor BOPA derivatives showed radical scavenging properties in H_2O_2 photolysis, implying that inhibition of the Cu(I)-induced Fenton reaction by both BTPA and BOPA analogues occurred predominantly through Cu(I)-chelation. In addition, NMR-monitored Cu(I)- and Zn(II)-titration of BTPA compounds **8** and **10** showed their high selectivity to a soft metal ion, Cu(I), as compared to a borderline metal ion, Zn(II). In summary, lipophilic BTPA analogues are promising highly selective Cu(I) ion chelators.

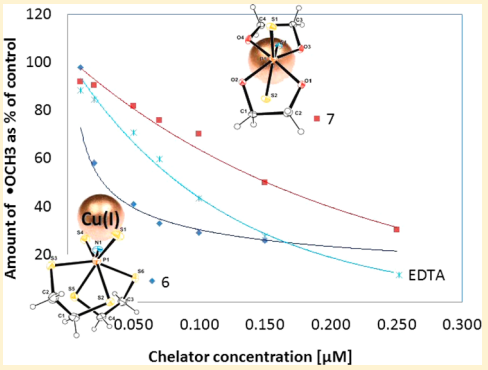

INTRODUCTION

Metal-ion chelators containing sulfur atoms have been suggested as a treatment for Alzheimer's and Wilson's diseases, as well as for heavy-metal poisoning (by soft metal ions such as Hg(II), Pb(II), and Cd(II)).[1] Dimercaptosuccinic acid and dimercaprol are used to treat heavy-metal poisoning by metal chelation and secretion through the urine.[2] Penicillamine[3] and 5′-nucleoside-phosphorthioate derivatives[4] have been proposed for the treatment for Wilson's and Alzheimer's disease, respectively. Related metal chelators containing sulfur atoms are also important for industrial uses as metal extractors[5] and lubricant additives.[6]

In the quest for new tools for chelation therapy and industrial applications that exhibit both high metal-ion affinity and selectivity, we recently prepared several bisphosphonate analogues bearing four sulfur atoms. Specifically, we synthesized O,O′-diester-methylene-diphonsphono-tetrathioate derivative **1**[7] and methylene diphosphonotetrathioate, MDPT, **2**, (Figure 1).[8] Compounds **1** and **2** were highly effective and selective soft/borderline metal-ion chelators. For instance, MDPT-Zn(II) complex was highly stable, log K 10.84, and was 10 000 000 times more stable than MDPT-Ca(II) complex. MDPT, **2**, was found to inhibit, via chelation, the Cu(I)-catalyzed Fenton reaction, Cu(I)/H_2O_2, (IC_{50} 26 μM) 2.5 times more potently than the Fe(II)-catalyzed Fenton reaction. Furthermore, **2** was 8 and 2.5 times more potent than glutathione (GSH) and EDTA in the Cu(I)/H_2O_2 system, respectively.[8] Analogue **1**, R = benzyl, proved to be a potent antioxidant (IC_{50} 53 μM), inhibiting, via chelation, the Cu(I)-catalyzed Fenton reaction at a 4-fold lower concentration than GSH. Analogue **1**, R = $CH_3(CH_2)_7$, inhibited the Fe(II)-catalyzed Fenton reaction at about the same concentration as ascorbic acid (IC_{50} 83 vs 93 μM).[7]

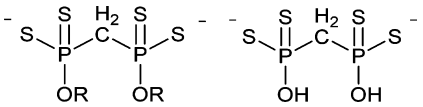

1 **2**

Figure 1. Structures of O,O′-diester-methylenediphosphonotetrathioate derivative **1** and methylene diphosphonotetrathioate (MDPT), **2**.

Received: March 4, 2014
Published: July 17, 2014

   dx.doi.org/10.1021/ic500465z | Inorg. Chem. 2014, 53, 7901−7908

The related metal-ion chelators, bis(dialkyl/aryl-phosphorothioyl)amide (BPA) analogues, **3a** (Figure 2),

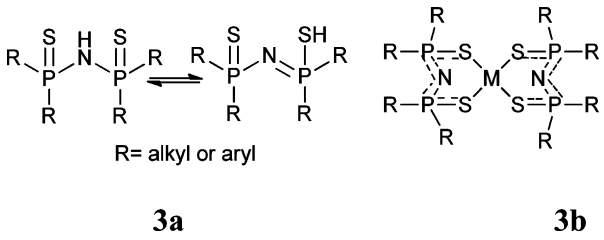

Figure 2. General structure of bis(dialkyl/aryl-phosphorothioyl)amide (BPA) derivatives, **3a**, and general structure of BPA-M^{2+} complex, **3b**.

allow delocalization of electrons and therefore are expected to be more polarizable than the corresponding bisphosphonate analogues.[9] BPA derivatives are soft/borderline metal ligands that bind a variety of metal ions (e.g., Zn(II),[10] Ni(II),[11,12] Cu(I)/(II),[13,14] and Mn(II)[15,16]). These compounds are versatile ligands, displaying a broad variety of coordination patterns leading to a great diversity of molecular and supramolecular structures.[17] Anions of BPA derivatives were usually found to be coordinated to a metal center by both sulfur atoms in a 2:1 ligand-to-metal ratio, thus leading to two six-membered MS4 inorganic chelate rings, **3b** (Figure 2).[16]

The geometry and stoichiometry of various neutral BPA ligand complexes with metal ions were studied.[16] For instance, the Zn(II) complex of BPA adopts a distorted tetrahedral geometry with a 2:1 ligand/metal ion ratio, **4**,[10] and BPA-Cu(I) complex, formed due to a redox reaction within $(BPA)_2^{2-}$-Cu(II) complex,[13,18] adopted multinuclear structures such as $[Cu_4L_3]^+$ and $[Cu_3L_3]$, **5a** and **b**,[9,19] respectively (Figure 3).

The affinity of bis(dialkyl/aryl-phosphorothioyl)amide to metal ions is used for metal extraction;[9,20] design of new materials, for example, long-lived, highly luminiscent lanthanide−imidodiphosphinate complexes with potential applications in photonic devices and sensors;[21] and treatment of antifungal[22] and antimicrobial infections.[23]

Here, we targeted to improve the soft metal-ion selectivity of the metal-ion chelator, **1**, by replacing its methylene bis(phosphonothioyl) scaffold by a bis(phosphorothioyl)amide moiety. Specifically, we synthesized a novel family of metal-ion chelators based on bis(1,3,2-dithia/dioxaphospholane-2-sulfide)amide (BTPA/BOPA) scaffolds, analogues **6**−**11**. We report on a novel synthetic approach for the preparation of these BTPA/BOPA chelators; X-ray crystal structures of the novel compounds; determination of geometries of BTPA/BOPA-M(II) complexes; evaluation of metal-ion binding mode by BTPA/BOPA derivatives; investigation of their antioxidant properties, and evaluation of their metal-ion selectivity.

RESULTS AND DISCUSSION

Design of Metal Ion Chelators Based on Bis(phosphorothioyl)amide Scaffold. We synthesized bis(phosphorothioyl)amide analogues bearing dithiaphospholane and dioxaphospholane rings **6**−**11** with a view to develop novel metal ion-selective chelators (Figure 4). Our design of the new chelators involved modification of three BPA moieties: (1) Addition of two sulfur atoms or two oxygen atoms on the phosphorus atom, aiming to tune the "soft" nature of the phosphorothioate moiety, and hence its metal-ion selectivity. (2) Inclusion of the phosphorothioate or phosphorotrithioate moiety into a five-membered ring, aiming to reduce degrees of freedom of the phosphorothioate moiety and help the correct orientation of the metal-coordinating atoms.[24,25] (3) Substituting ethyl or benzyl groups on the bridging nitrogen atom (or having a bridging nitrogen anion), aiming to tune solubility and to add M^{2+} coordination sites (in the cases of benzyl and nitrogen anion as in **6**/**7**).

Synthesis of BTPA/BOPA Derivatives 6−11. The synthesis of derivatives **6**−**11** was achieved by reaction of 2 equiv of 2-chloro-1,3,2-dithia(dioxa)phospholane **12a**,**b** with various amines in tetrahydrofuran (THF) at −78 °C to room temperature (RT), to form the dithia(dioxa)phospholane derivatives **13a**,**b** (Scheme 1). The formation of intermediates **13a**,**b** was verified by $^{31}P/^{1}H$ NMR. Intermediates **13a**,**b** were then treated with elemental sulfur, S_8, in pyridine at −78 °C to obtain the oxidized bis(phosphorothioyl)amide analogues **6**−**11**.

Compounds **6** and **7** were obtained as pure white solids upon filtration of the reaction mixtures and crystallization of the yellowish oily residue in hot EtOH. Compound **6** was obtained at a 69% yield (^{31}P NMR: 75.1 ppm), and compound **7** was obtained at a 91% yield (^{31}P NMR: 69.6 ppm). Compounds **8** and **9** were crystallized from $CHCl_3$/*n*-hexane to give yellowish solids that, after successive washings with CS_2, provided pure white solids. Compounds **8** and **9** were obtained at a 77% yield (^{31}P NMR: 102.8 ppm) and a 45% yield (^{31}P NMR: 87.1 ppm), respectively. Compound **10** was crystallized from $CHCl_3$ to give a white solid at a 60% yield (^{31}P NMR: 108 ppm). Compound **11** was obtained upon separation over silica gel column with hexane/EtOAc to give a white solid at a 30% yield (^{31}P NMR: 86.4 ppm).

X-ray Crystal Structures of BTPA/BOPA Analogues 6, 7, and 8. Single crystals of analogues **6** and 7 were obtained by slow perfusion of ether into dichloromethane (DCM) solutions

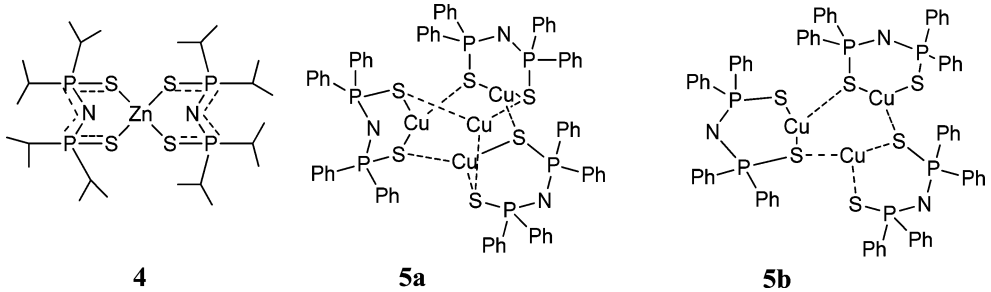

Figure 3. Examples of BPA derivatives forming metal complexes with various geometries: Zn(bis(di-iPr-phosphorothioyl)amide)$_2$, **4**, $Cu_4((Ph_2(S)P)_2N)_3$, **5a**, and $Cu_3((Ph_2(S)P)_2N)_3$, **5b**.

dx.doi.org/10.1021/ic500465z | Inorg. Chem. 2014, 53, 7901−7908

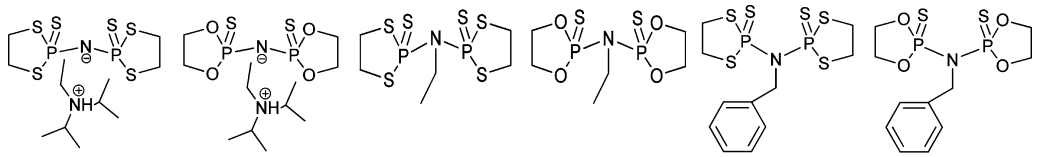

6 7 8 9 10 11

Figure 4. Structures of BPTA and BOPA Analogues **6**–**11**.

Scheme 1. Synthesis of BPTA and BOPA Analogues 6–11

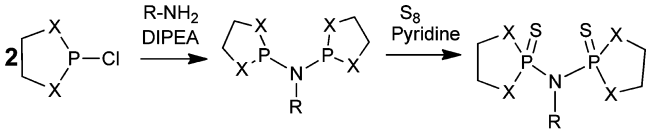

12 **13** **6-11**

12a. X = S **13a**. X = S, R= H, ethyl, benzyl
12b. X = O **13b**. X = O, R= H, ethyl, benzyl

of compounds **6** and **7**. Compound **8** was crystallized from chloroform by slow evaporation of the solvent. The structures of compounds **6**, **7**, and **8** were solved by X-ray diffraction. Compound **6** exhibited *gauche* conformation between P1═S1/P2═S4 moieties (Figure 5A), consistent with that reported for $^{i}Pr_2P(S)NHP(S)^{i}Pr_2$.[10] The average P═S and P−N bond lengths of **6** were 1.960 and 1.593 Å, respectively. Likewise, compound **8** exhibited *gauche* conformation between P1═S3/P2═S6 (Figure 5B), and the average P═S and P−N bond lengths were 1.938 and 1.698 Å, respectively. Surprisingly, the crystal structure of compound **7** indicated an *anti*-conformation with P1═S1/P2═S2 moieties inverted to each other (Figure 5C). The average P−N bond length for compounds **6** and **7** was 1.587 Å, while for compound **8** it was 1.698 Å. These differences are attributed to electron delocalization in compounds **6** and **7** over SPNPS atoms. Selected bond lengths and angles are listed in Table 1.

Previously we reported the crystal structure of the related PCP-based compound methylene-bis(1,3,2-dithiaphospholane-2-sulfide), **14** (Figure 6).[7] A *gauche* conformation was observed between the two dithiaphospholane rings. The average P═S and P−C bond lengths were 2.044 and 1.827 Å, respectively, longer than P═S and P−N bonds in **6**–**8** due to the lack of electron delocalization in **14**.

In both crystal structures of PNP-based analogues **6** and **8** and the corresponding PCP-based analogue **14**, the dithiophospholane rings dictated *gauche* configuration, while in the PNP-based compound **7**, dioxaphospholane rings forced an *anti* conformation. The difference of conformation between **6** and **7** is possibly due to the larger dipole in P−O versus P−S bond (Δ electronegativity 1.3 vs 0.3, respectively), resulting in dipole repulsion and an *anti* conformation in compound **7**.

To study metal-ion chelation by BTPA and BOPA analogues, we first formed metal complexes of **6** and **7** with Zn(II), Hg(II), and Ni(II) in ethanol at a 2:1 ligand-to-metal ion ratio. Complexes of compound **6** with Zn(II), Hg(II), or Ni(II) precipitated from ethanolic solution. Hg(II) and Ni(II) complexes were insoluble in any organic and aqueous media. Addition of Hg(II) or Ni(II) to compound **7** resulted in a black paste or a brownish solid, respectively. A Zn(II) complex with **7** was soluble in ethanol. Solid complexes of chelators **6** or **7** with Hg(II), Ni(II), or Zn(II), were investigated by solid-state NMR spectroscopy applying the magic-angle spinning (MAS) method. First, a ^{31}P-MAS NMR spectrum of the free chelator **6** was measured (Figure 7a). The chelator isotropic (iso) signals are found at 69.4 ppm, J = 255 Hz, in addition to six aniso signals. In the ^{31}P-MAS NMR spectrum of **6**-Hg(II) complex (Figure 7b) the iso signals move downfield to 83.4 ppm, and the iso signals are in 1:1 ratio that may be attributed to a square planar[26] or tetrahedral geometry.[9] The two aniso signals are barely seen due to the micro crystalline solid and the

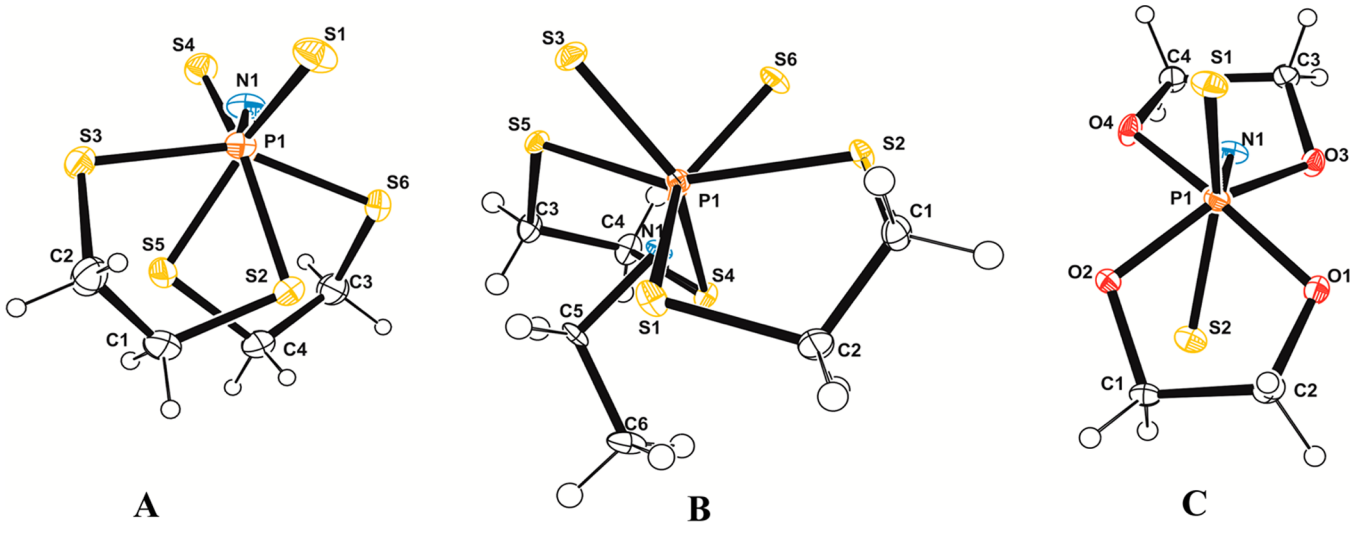

Figure 5. Structures of BTPA and BOPA analogues (A) **6**, (B) **8**, and (C) **7**, shown in a Newman projection (50% ellipsoid probability). The counter cations of compounds **6** and **7** were omitted for clarity.

dx.doi.org/10.1021/ic500465z | *Inorg. Chem.* 2014, 53, 7901−7908

Table 1. Selected Bond Lengths and Angles of Compounds 6, 7, and 8

compound	atoms	length [Å]	atoms	angle [deg]
6	S(1)−P(1)	1.9635(13)	S(1)−P(1)−S(3)	113.83(5)
6	P(1)−S(3)	2.1025(13)	S(1)−P(1)−N(1)	111.0(1)
6	P(1)−S(2)	2.1158(13)	S(2)−P(1)−S(3)	98.52(5)
6	P(1)−N(1)	1.597(3)	S(5)−P(2)−S(6)	97.96(6)
7	S(1)−P(1)	1.9631(10)	S(1)−P(1)−O(1)	112.54(8)
7	P(2)−O(3)	1.621(2)	S(2)−P(2)−O(3)	110.8(8)
7	P(1)−O(2)	1.6113(19)	O(1)−P(1)−O(2)	96.6(1)
7	P(1)−N(1)	1.572(2)	O(3)−P(2)−O(4)	96.3(1)
8	P(1)−S(3)	1.9410(5)	S(2)−P(1)−N(1)	112.74(5)
8	S(1)−P(1)	2.0768(5)	S(1)−P(1)−S(3)	110.16(2)
8	P(1)−S(2)	2.1085(5)	S(2)−P(1)−S(3)	119.73(2)
8	P(1)−N(1)	1.7124(13)	S(5)−P(2)−S(6)	112.16(2)

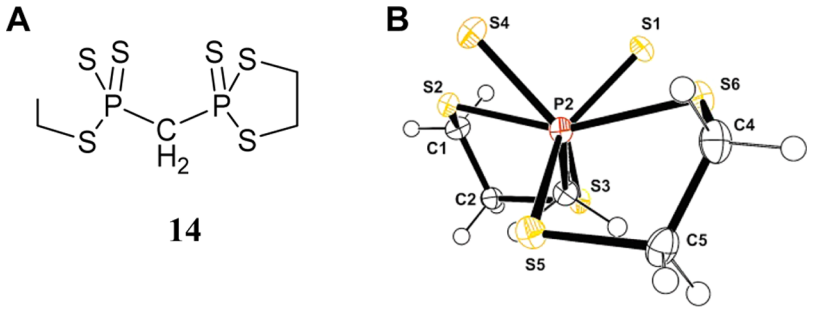

Figure 6. (A) Methylene-bis(1,3,2-dithiaphospholane-2-sulfide), **14**. (B) X-ray crystal structure of **14**.[7]

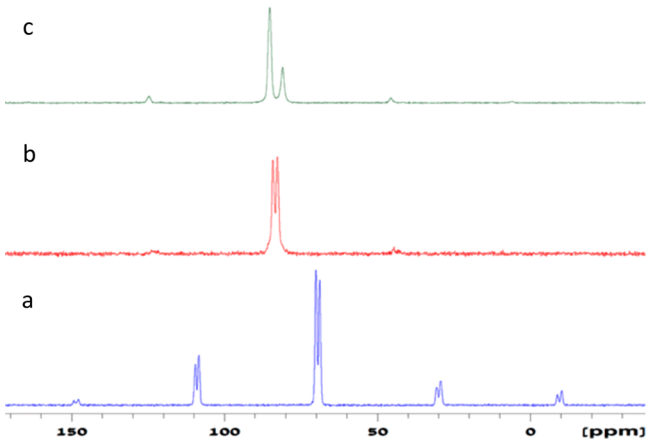

Figure 7. ^{31}P-MAS NMR spectra at 202 MHz. (a) Compound **6**. (b) **6**-Hg(II) complex. (c) **6**-Zn(II) complex.

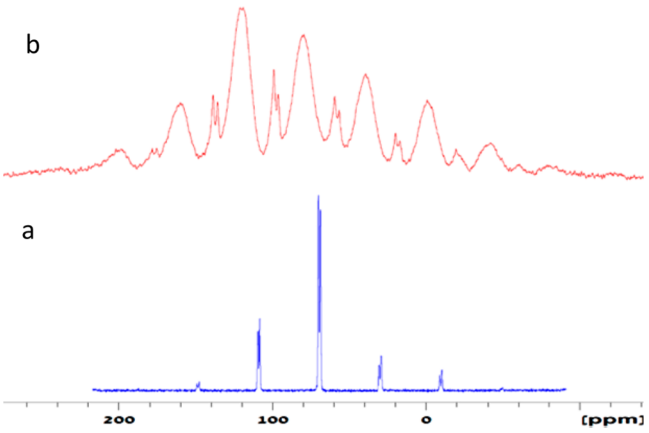

Figure 8. ^{31}P-MAS NMR spectra at 202 MHz. (a) Compound **6**. (b) **6**-Ni(II) complex.

complex geometry dictated by the metal ion. Zn(II)-**6** complex exhibited two iso signals at 83.1 ppm in a 3:1 ratio, which is characteristic of a distorted tetrahedral geometry (Figure 7c).[16] Changes in the dithiaphosphalane rings due to M(II) coordination were observed by ^{13}C-MAS NMR as well (Supporting Information, Figure S1).

The ^{31}P-MAS NMR spectrum of **6**-Ni(II) exhibits broad signals (Figure 8b), unlike the narrow signals of spectra of **6**-Zn(II) and **6**-Hg(II) ion complexes. The broad aniso signals may possibly be attributed to a polymeric structure.

Similarly to the case of **6**, the ^{31}P-MAS NMR spectrum of compound **7** (Supporting Information, Figure S2) exhibits iso peaks at 74 ppm, J = 1250 Hz, and an aniso pattern, and the spectrum of **7**-Ni(II) complex exhibits very large anisotropy signals, possibly due to a polymeric structure.

BTPA Analogues Prefer Cu(I) Versus Fe(II) Chelation. We indirectly studied Cu(I) and Fe(II) chelation by BTPA and BOPA analogues, by assessing their antioxidant capacity in Fenton reactions. Specifically, we monitored, using electron paramagnetic resonance (EPR), their ability to modulate $OH^{\bullet}$ radical formation from H_2O_2 in Fe(II)/Cu(I)-induced Fenton reaction. Because of insolubility of these compounds in water, all analogues were dissolved in dimethyl sulfoxide (DMSO). α-Phenyl N-tertiary-butyl nitrone (PBN) was used as a radical spin trap.[27] The hydroxyl radical generated by Fenton reaction is converted into a methyl radical via its reaction with DMSO, which undergoes oxidation under aerobic conditions to produce methoxy radical $OCH_3^{\bullet}$.[27] The long-lived PBN/$OCH_3^{\bullet}$ adduct was then detected by EPR. The addition of chelators to Fe(II)/Cu(I)-H_2O_2 mixture lowered the PBN/$OCH_3^{\bullet}$ signal due to metal-ion chelation and/or radical

dx.doi.org/10.1021/ic500465z | Inorg. Chem. 2014, 53, 7901−7908

scavenging (Figure 9).[28] The inhibition of radical production by compounds **6**–**11**, expressed in IC_{50} values, was compared

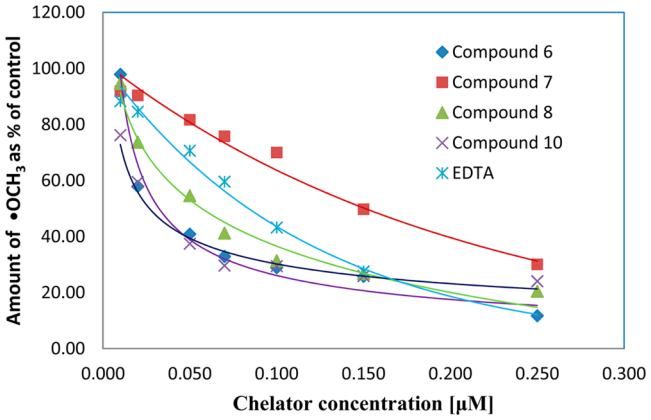

Figure 9. Inhibition of OH radical formation in Cu(I)/H_2O_2 system by derivatives, **6**, **7**, **8**, and **10** vs EDTA, as reflected by the relative amount of $OCH_3^•$.

to the inhibitory effect of a metal-ion chelator, ethylenediaminetetraacetic acid (EDTA) (Table 2).

Table 2. Inhibition of Fe(II)/Cu(I)-Induced Fenton Reaction by Analogues 6–11 Versus EDTA

	IC_{50} [μM][a]	
compound	Fe(II)	Cu(I)
6	>500 μM	32 ± 1
7	>500 μM	160 ± 6
8	>500 μM	56 ± 4
9	>500 μM	>500 μM
10	>500 μM	29 ± 0.8
11	>500 μM	>500 μM
EDTA	77 ± 1	86 ± 4

[a] IC_{50} values represent the compound concentration that inhibits 50% of the $OCH_3^•$ radical amount produced in the control reaction. The latter includes Cu(I)/Fe(II)-H_2O_2 in DMSO in the presence of PBN.

The best antioxidant activity was measured for the dithiaphospholane compounds **6**, **8**, and **10**, with IC_{50} values of 32, 56, and 29 μM, respectively (Table 2). These results meet the expected, since those compounds have a much "softer" character than dioxaphospholane compounds **7**, **9**, and **11**, due to the presence of six sulfur atoms versus two sulfur atoms in the latter compounds. An appealing explanation for the reduced activity of **7**, **9**, and **11** is that the electronegative oxygen atoms, unlike sulfur atoms, withdraw electrons from the SPNPS chelating system to the dioxaphosphospholane rings. The poor electron availability of the SPNPS moiety reduces chelation of metal ions. Yet, the presence of oxygen atoms significantly affects also the conformation of the BOPA analogue (Figure 5). In dioxaphospholane analogue **7**, the sulfur atoms are arranged in an *anti*-conformation, thus making the Cu(I) chelation less effective as compared to *gauche* conformation in dithiaphospholane **6**. Indeed, compound **6** was 5 times more potent than compound **7** (32 vs 160 μM, respectively) although both share the same charge delocalization on the SPNPS moiety.

Substitution of a benzyl group on the central BTPA nitrogen atom resulted in the best antioxidant studied here, compound **10**, being 3-fold more active than EDTA (29 vs 86 μM). Compound **10** was a 2-fold more potent antioxidant than compound **8** possibly due to additional π-cation interactions between the aromatic ring and Cu(I).

Interestingly, in the Fe(II)-H_2O_2 system, we could not determine IC_{50} values for BTPA/BOPA compounds because the minimal amount of radical production exceeds 50% even at 500 μM BTPA/BOPA analogue. On the other hand, in Cu(I)-H_2O_2 system all BTPA analogues inhibited OH radical production. This observation indicates the clear selectivity of BTPA compounds to Cu(I) versus the borderline Fe(II) ion.

BTPA Analogues Are Cu(I) Chelators and Not Radical Scavengers. Since Fenton reaction can be inhibited by both metal-ion chelation and/or radical scavenging, we also evaluated analogues **6**–**11** as potential radical scavengers. We produced OH radicals by photolysis of H_2O_2 with UV radiation[29] and monitored radical scavenging by compounds **6**–**11** using EPR. The radical scavenging activity was determined as a function of the antioxidant concentration and was calculated relative to a control measurement, which is the maximal production of OH radical via photolysis of H_2O_2, in the absence of a scavenger. The experiment conditions were the same as for the above-mentioned Fenton reaction inhibition experiment except for the absence of the metal ion. The mixture was irradiated (at 365 nm) for 2 min with a UV lamp followed by EPR measurement. The inhibition of radical

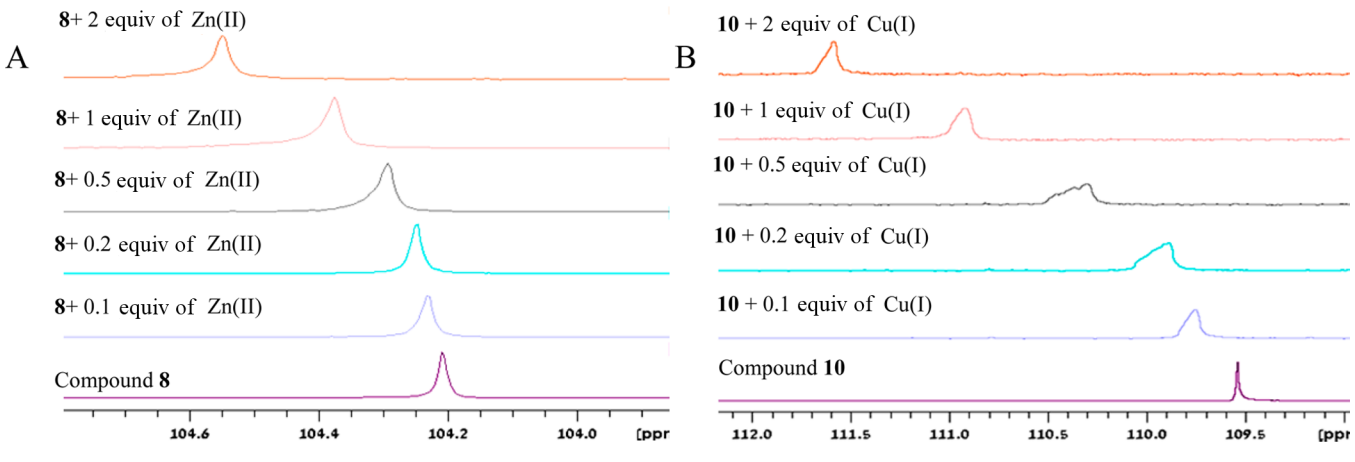

Figure 10. ^{31}P NMR spectra in DMSO-d_6 of (A) **8**-Zn(II) complex and (B) **10**-Cu(I) complex at 241 MHz.

dx.doi.org/10.1021/ic500465z | Inorg. Chem. 2014, 53, 7901–7908

production by compounds **6**−**11** was compared to the inhibitory effect of the known radical scavenger Trolox.[30]

All compounds showed no radical scavenging activity, even at high ligand concentration (>500 μM). This finding indicates that the mechanism of action of BTPA/BOPA analogues as antioxidants involves chelation, namely, capturing the metal ion and preventing electron transfer from Cu(I), thus inhibiting the production of hydroxyl/methoxyl radicals.

BTPA Analogues 8 and 10 Chelate Preferentially Cu(I) Versus Zn(II). The above EPR data showed that BTPA analogues **6**, **8**, and **10** were most potent and Cu(I)-selective antioxidants acting by Cu(I)-chelation rather than radical scavenging. To establish the mode of borderline versus soft metal-ion chelation by these analogues, we titrated compound **8** with either Zn(II) or Cu(I) ions and monitored the titration by $^{31}P/^{1}H$ NMR in DMSO-d_6.

Upon the addition of $ZnCl_2$ (dissolved in D_2O) the ^{31}P NMR signal of **8** at 104 ppm neither shifted nor broadened significantly. The maximal shift measured upon the addition of 2 equiv of $ZnCl_2$ was 0.3 ppm (Figure 10A). Hence, it appears that there is an indirect chelation of Zn(II) by the ligand, causing an insignificant shift in ^{31}P NMR spectrum. ^{1}H NMR showed no change even upon the addition of up to 2 equiv of Zn(II).

We repeated the above NMR-monitored metal-ion titration, this time with $(Cu(I)(CH_3CN)_4PF_6)$ solution in CD_3CN. Addition of up to 0.1−0.5 equiv of Cu(I) neither changed the chemical shift of phosphor and proton signals of analogue **8** nor broadened those signals (Supporting Information, Figure S3). However, upon addition of 1 equiv of Cu(I), the phosphor signal shifted from 104.2 to 105.5 ppm, and its width broadened dramatically.

Next, we titrated compound **10** with Cu(I) (Figure 10B). Again, no change was observed in the ^{1}H NMR spectra; however, in the ^{31}P NMR spectra the phosphor signal shifted and broadened, even upon addition of 0.1 equiv of Cu(I). After an addition of 0.5−2 equiv of Cu(I), the signal broadened and shifted from 109.5 to 111.5 ppm, a more significant change than that observed for compound **8** (Supporting Information, Figure S3). Yet, the shift of chemical shift, $\Delta\delta$, of compound **10** is still small as compared to that observed for a related BPA analogue, $^{i}Pr_2(S)PNHP(S)^{i}Pr_2$,[10] where a $\Delta\delta$ value of ca. 30 ppm was observed upon coordination of Zn(II). This phenomenon may be because this BPA analogue is negatively charged, whereas analogues **8** and **10** are neutral ligands.

Thus, solution NMR data indicated the preference of **8** for Cu(I) versus Zn(II) and that chelation of Cu(I) ion occurred through the $(R_2S)PS$ moiety, whereas Zn(II) coordination occurred possibly via bridging water molecules. In addition, in compound **10**, Cu(I) is possibly coordinated also by the phenyl group via π-cation interactions.

CONCLUSIONS

Bis(1,3,2-dithia/dioxaphospholane-2-sulfide)amide (BTPA/BOPA) analogues **6**−**11** were synthesized via a new and efficient synthetic methodology. Crystal structures of BTPA compounds **6** and **8** revealed a *gauche* geometry, while BOPA compound **7** exhibited an *anti* geometry. Solid-state ^{31}P-MAS NMR spectra of **6**-Hg(II) and **6**- Zn(II) complexes imply a square planar or tetrahedral geometry of the former and a distorted tetrahedral geometry of the latter. The ^{31}P-MAS NMR spectra of both **6**-Ni(II) and **7**-Ni(II) complexes suggest a polymeric structure.

Unlike BOPA analogues, BTPA analogues **6**, **8**, and **10** were found to be potent antioxidants inhibiting OH radical production in Cu(I)-H_2O_2 Fenton system (IC_{50} 32, 56, and 29 μM, respectively). Both BTPA and BOPA analogues **6**−**11** were extremely poor antioxidants in Fe(II)-H_2O_2 system. None of the derivatives **6**−**11** showed radical scavenging properties, which led us to conclude that inhibition of OH radical production occurred predominantly through metal-ion chelation. The selectivity of BTPA to Cu(I) versus Fe(II) exceeded 20-fold. The reduced antioxidant activity of BOPA analogues **7**, **9**, and **11** is possibly due not only to oxygen atoms, which withdraw electrons from the SPNPS chelating system, but also to an *anti* conformation of the P═S moieties, thus making metal-ion chelation less effective versus dithiaphospholane-sulfide derivatives **6**, **8**, and **10** arranged in a *gauche* conformation.

Solution NMR-monitored Cu(I) and Zn(II) titration of compounds **8** and **10** revealed high selectivity for a soft metal ion, Cu(I), versus a borderline metal ion, Zn(II), with the former being directly coordinated via a $(R_2S)PS$ moiety, and the latter possibly via bridging water molecules. Although sharing similar potency (IC_{50} values) with MDPT, **2**, compound **10** proved to be by far more selective to Cu(I) versus Fe(II) (≫ 20-fold vs 2.5-fold). Likewise, BTPA analogues were found to be more effective Cu(I)- chelators than the related lipophilic MDPT−diester chelators, **1**.[7] Furthermore, MDPT is prone to air-oxidation,[8] whereas BTPA is highly stable under these conditions.

In summary, in this study, we successfully developed a novel class of stable, lipophilic BTPA chelators that are highly Cu(I)-selective versus borderline ions such as Zn(II) and Fe(II).

EXPERIMENTAL SECTION

General. All air- and moisture-sensitive reactions were carried out in flame-dried, N_2-flushed, two-neck flasks sealed with a rubber septum, and the reagents were introduced with a syringe. All commercial reagents were used without further purification, unless otherwise noted. All reactants in moisture-sensitive reactions were dried overnight in a vacuum oven. Diisopropyl ethyl amine (DIPEA) was distilled from CaH_2. Pyridine was distilled from KOH. THF was distilled from sodium in the presence of benzophenone, and benzyl amine was distilled from NaOH. $Cu(CH_3CN)_4PF_6$ was purified before use by dissolving the salt in acetonitrile (HPLC grade) and filtering the unsoluble Cu(II) salt. The filtrate was flushed with argon stream. The concentration of the Cu(I) salt was determined by UV spectroscopy by the addition of a specific Cu(I) indicator, bicinchoninic acid (BCA) (ε562 = 7700 M^{-1}).[31] Progress of reactions was monitored by thin-layer chromatography on precoated Merck silica gel plates (60F-254). Visualization was accomplished by UV light. ^{1}H NMR and ^{31}P NMR spectra were measured with Bruker DPX-300 (300 MHz for ^{1}H), AC-200 (80.3 MHz for ^{31}P), or DMX-600 (600 and 240.9 MHz for ^{1}H and ^{31}P, respectively) spectrometers. High-resolution mass spectra (HR-MS) were recorded on an AutoSpec-E FISION VG mass spectrometer by chemical ionization and a high-resolution matrix-assisted laser desorption ionization time-of-flight mass spectrometer (MS-MALDI-TOF) with autoflex TOF/TOF instrument (Bruker, Germany). Analysis of the amount of OH radicals produced in Cu(I) and Fe(II)-H_2O_2/tested compound systems was performed by solution EPR spectroscopy using a Bruker ER 100d X-band spectrophotometer. The spectra were processed by Bruker WIN-EPR software version 2.11. The signal intensities were evaluated by integration of the second signal of the PBN−$OCHH_3$ spin adducts and reported as percentage of the control (the signal intensity obtained without the addition of tested compound).

Typical Procedure for the Synthesis of *N*-ethyl-*N*-isopropyl-propan-2-aminium-bis(2-sulfido-1,3,2-dithiaphospholan-2-yl)-

dx.doi.org/10.1021/ic500465z | Inorg. Chem. 2014, 53, 7901−7908

amide, 6, and *N*-ethyl-*N*-isopropylpropan-2-aminium-bis(2-sulfido-1,3,2-dioxaphospholan-2-yl)amide, 7. 2-Chloro-1,3,2-dithiaphospholane, **12a**, or 2-chloro-1,3,2-dioxaphospholane, **12b**, (11.23 mmol) in dry THF (4 mL) was cooled to −78 °C. Dry DIPEA (1.45 g, 11.23 mmol) was added dropwise so that reaction temperature did not exceed −45 °C, followed by a slow addition of 0.5 M NH_3 solution in THF (45 mL, 22.46 mmol). After 0.5 h at −78 °C, the temperature was raised to RT for another 0.5 h. ^{31}P NMR analysis of the reaction mixture indicated that the reaction was completed. The mixture was cooled to −78 °C, and dry DIPEA (1.45 g, 11.23 mmol) was added followed by a slow addition of **12a** or **12b** (11.23 mmol). The reaction was stirred at RT overnight. ^{31}P NMR showed that the reaction was completed. The mixture was cooled to −78 °C, dry pyridine (8 mL) and S_8 (0.77 g, 24.06 mmol) were added, and the temperature was raised to RT. After an additional 2 h, ^{31}P NMR indicated the formation of compound **6** or **7**. The mixture was vacuum filtered, and the filtrate was evaporated to give yellowish oil. The oil was crystallized by dissolving it in hot EtOH. The clear mixture was cooled to RT and then cooled to −78 °C to obtain a white solid. The solid was filtered, washed with cold EtOH, and dried under vacuum to give a white solid. Compound **6** was obtained at a 69% yield (3.52 g). mp 146 °C. ^{1}H NMR (600 MHz, $CDCl_3$): δ 3.95 (sep, J = 6.7 Hz, 2H), 3.74−3.64 (m, 4H), 3.64−3.57 (m, 4H), 3.29 (q, J = 7.61 Hz, 2H), 1.53−1.43 (m, 15H) ppm. ^{13}C NMR (150 MHz, $CDCl_3$): δ 54.9, 42.9, 41.6, 19.3, 18, 12.2 ppm. ^{31}P NMR (243 MHz, $CDCl_3$): δ 75.1 ppm. HR-MS (MALDI) m/z calcd for $C_4H_8NP_2S_6$ $[M - C_8H_{20}N]^-$: 323.846, found: 323.848. Fourier transform infrared (FT-IR) attenuated total reflection (ATR): 2984w, 2912w, 2691w, 1457w, 1414w, 1177s, 1143m, 938w, 614vs cm^{-1}. Compound **7** was obtained at a 91% yield (4 g). mp 105 °C. ^{1}H NMR (600 MHz, $CDCl_3$): 4.34−4.24 (m, 8H), 3.94 (sep, J = 6.7 Hz, 2H), 3.32 (q, J = 7.44 Hz, 2H), 1.52−1.46 (m, 15H) ppm. ^{13}C NMR (150 MHz, $CDCl_3$): 63.5, 55.1, 43.0, 18.7, 12. ^{31}P NMR (243 MHz, $CDCl_3$): 69.6 ppm. HRMS (MALDI) m/z calcd for $C_4H_{10}NO_4P_2S_2$ $[M + H - C_8H_{19}N]^+$: 261.952, found: 261.951. FT-IR (ATR): 2974w, 2699w, 1466w, 1235m, 1024s, 917m, 807m, 761m, 664m cm^{-1}.

2,2′-(Ethylazanediyl)bis(1,3,2-dithiaphospholane-2-sulfide), 8. 2-Chloro-1,3,2-dithiaphospholane, **12a** (3.06 g, 19.29 mmol), in dry THF (8 mL), was cooled to −78 °C. Dry DIPEA (2.49 g, 19.29 mmol) was slowly added followed by the addition of 2 M ethylamine in THF (0.44 g, 9.65 mmol). The mixture was stirred at RT overnight. ^{31}P NMR of the reaction mixture indicated the formation of **13a** (^{31}P NMR: 106 ppm). Pyridine (8 mL) and S_8 (1.32 g, 41.25 mmol) were added to a mixture of **13a** at −78 °C, the mixture was allowed to reach RT, and after 2 h the mixture was vacuum filtered. The filtrate was evaporated to give yellowish oil that was dissolved in DCM (20 mL) and washed with water and a saturated solution of $NaHCO_3$ and NaCl. Finally, the solution was dried over Na_2SO_4 and evaporated to give yellowish oil. The oil was crystallized from $CHCl_3$/*n*-hexane to give a yellowish solid that, after successive washings with CS_2, provided a pure white solid, which was dried in air. Compound **8** was obtained in 77% yield (2.63 g). mp 154 °C. ^{1}H NMR (600 MHz, acetone-d_6): 3.9−3.7 (m, 10H), 1.04 (t, J = 7.1 Hz, 3H) ppm. ^{13}C NMR (150 MHz, acetone-d_6): 47.7, 42.6, 16.8. ^{31}P NMR (243 MHz, acetone-d_6): 102.8 ppm. HR-MS (MALDI) m/z calcd. for $C_6H_{14}NP_2S_6$ $[M + H]^+$: 353.892, found: 353.889. FT-IR (ATR): 2989w, 2952w, 2922w, 1438w, 1409w, 1290w, 1147w, 1031m, 925m, 861m, 748m, 663s cm^{-1}.

2,2′-(Ethylazanediyl)bis(1,3,2-dioxaphospholane-2-sulfide), 9. The reaction was performed following the above-mentioned procedure for the synthesis of compound **8**. The product was obtained from **12b** (1.42 g, 11.23 mmol) as a white powder in 45% yield (0.73 g). mp 105 °C. ^{1}H NMR (600 MHz, $CDCl_3$): 3.02−2.96 (m, 10H), 1.19 (t, J = 7.1 Hz, 3H) ppm. ^{13}C NMR (150 MHz, $CDCl_3$): 65.93, 37.02, 16.8 ppm. ^{31}P NMR (243 MHz, $CDCl_3$): 87.16 ppm. HR-MS (MALDI) m/z calcd. for $C_6H_{14}NO_4P_2S_2$ $[M + H]^+$: 289.984 found 290.951. FT-IR (ATR): 2989w, 2952w, 2922w, 1438w, 1409w, 1290w, 1147w, 1031m, 925m, 861m, 748m, 663s cm^{-1}.

2,2′-(Benzylazanediyl)bis(1,3,2-dithiaphospholane-2-sulfide), 10. 2-Chloro-1,3,2-dithiaphospholane, **12a** (2.95 g, 18.66 mmol), in dry THF (8 mL), was cooled to −78 °C. Dry DIPEA (2.41 g, 18.66 mmol) was slowly added followed by the addition of dry benzylamine (1 g, 9.33 mmol). The mixture was stirred at RT overnight. After 24 h pyridine (8 mL) and S_8 (0.657 g, 20.52 mmol) were added to the mixture at −78 °C to obtain a light yellow turbid suspension. The mixture was allowed to reach RT, and after 2 h the mixture was vacuum filtered. The filtrate was evaporated to give yellowish oil that was dissolved in DCM (20 mL) and washed with water and a saturated solution of $NaHCO_3$ and NaCl. Finally, the solution was dried over $MgSO_4$ and evaporated to give yellowish oil. The organic phase was crystallized from $CHCl_3$ to give a white solid in 60% yield (2.3 g). mp 150 °C. ^{1}H NMR (400 MHz, $CDCl_3$): 7.46−7.36 (m, 5H), 5.01 (t, J = 20 Hz, 2H), 3.62−3.43 (m, 8H) ppm. ^{13}C NMR (100 MHz, $CDCl_3$): 137.0, 128.4, 127.6, 127.4, 53.6, 41.9 ppm. ^{31}P NMR (162 MHz, $CDCl_3$): 108.03 ppm. HR-MS (Cl) m/z calcd. for $C_{11}H_{16}NP_2S_6$ $[M + H]^+$: 415.908, found: 415.911. FT-IR (ATR): 2963w, 1494w, 1448s, 1412w, 1353w, 1281w, 1244w, 1149m, 1023s, 1001m, 938m, 737s cm^{-1}.

2,2′-(Benzylazanediyl)bis(1,3,2-dioxaphospholane-2-sulfide), 11. 2-Chloro-1,3,2-dioxaphospholane, **12b** (2.13 g, 16.84 mmol), in dry THF (8 mL), was cooled to −78 °C. Dry DIPEA (1.98 g, 15.30 mmol) was slowly added followed by the addition of dry benzylamine (0.82 g, 7.65 mmol). The mixture was stirred at RT overnight. After 24 h pyridine (8 mL) and S_8 (0.539 g, 16.83 mmol) were added to the mixture at −78 °C to obtain a light yellow turbid suspension. The mixture was allowed to reach −15 °C, and after 2 h the mixture was vacuum filtered. The filtrate was evaporated to give yellowish oil that was dissolved in DCM (20 mL) and washed with water and a saturated solution of $NaHCO_3$ and NaCl. Finally, the solution was dried over Na_2SO_4 and evaporated to give yellowish oil. The crude product was separated over silica gel column chromatography, hexane/EtOAc (60%:40%), to give a white solid in 30% yield (0.8 g). mp 145 °C. ^{1}H NMR (600 MHz, $CDCl_3$): 7.48−7.26 (m, 5H), 4.97 (t, J = 16.8 Hz, 2H), 4.42−4.22 (m, 8H) ppm. ^{13}C NMR (150 MHz, $CDCl_3$): 137.8, 128.5, 127.9, 127.8, 66.5, 53.4 ppm. ^{31}P NMR (243 MHz, $CDCl_3$): 86.43 ppm. HR-MS (Cl) m/z calcd. for $C_{11}H_{16}NO_4P_2S_2$ $[M + H]^+$: 351.999, found: 351.996. FT-IR (ATR): 2970w, 2905w, 1494s, 1457w, 1317w, 1230w, 1202w, 1031m, 1011m, 1001s, 924m, 822s, 791s, 773s, 734s, 695s, 651m, 625m cm^{-1}.

Evaluation of Inhibition of OH Radical Production in Fenton Reactions by BPA Analogues 6−11 Using EPR. EPR settings for OH radical detection were as follows: microwave frequency, 9.76 GHz; modulation frequency, 100 kHz; microwave power, 6.35 mW; modulation amplitude, 1.2 G; time constant, 655.36 ms; sweep time, 83.89 s; and receiver gain, 2×10^5 in experiments with Cu(I) and Fe(II).

Fenton Reaction Monitored by EPR Using PBN as a Radical Spin Trap. $Cu(CH_3CN)_4PF_6$ (2 mM) in acetonitrile (10 μL) or 0.5 mM $FeCl_2 \cdot 4H_2O$ in DMSO (10 μL) were added to 5−500 mM tested compound in DMSO (10 μL). Afterward, DMSO (60−70 μL) was added to the mixture. After mixing for 2 s, 50 mM PBN (10 μL) in DMSO (1 mL) was quickly added followed by the addition of 100 mM H_2O_2 (10 μL). Each EPR measurement was performed 150 s after the addition of H_2O_2. All experiments were performed at room temperature, in a final volume of 100 μL.

Photolysis of H_2O_2. EPR settings for OH radical detection were as described above. The sample, composed of 5−500 μM tested compound (1−10 μL), was followed by an addition of DMSO (70−80 μL). 50 mM PBN (10 μL) was quickly added followed by the addition of 100 mM H_2O_2 (10 μL) to the mixture. A short mixing of the sample was performed after the addition of each component. The sample was then irradiated for 2 min with a UV lamp (model VL-315 BL, wavelength: 365 nm, power: 30 W, Vilber Lourmat, Marne-la-Vallée, France) and was immediately transferred to a narrow Teflon tube for EPR measurement. The control measurement composed from DMSO (80 μL), PBN (10 μL), and H_2O_2 (10 μL) excluding the ligand. All experiments were performed in triplicate at RT, in a final volume of 100 μL.

Identification of Metal Ion Binding Sites by ^{31}P/^{1}H NMR Measurements. *Titration of Compound 8 by Zn(II).* $ZnCl_2$ (0.1−2

dx.doi.org/10.1021/ic500465z | Inorg. Chem. 2014, 53, 7901−7908

equiv) in D_2O solution was added to compound **8** (1.27 mg, 0.0036 mmol) in DMSO-d_6 (0.6 mL), and $^1H/^{31}P$ NMR spectra were measured at 200 and 81 MHz, respectively.

*Titration of Compounds **8** and **10** by Cu(I).* $Cu(CH_3CN)_4PF_6$ was purified before use by dissolving the salt in acetonitrile-d_3 and filtering the unsoluble Cu(II) salt. The filtrate was flushed with argon stream to dryness. The concentration of the Cu(I) salt was determined by UV spectroscopy by the addition of the specific Cu(I) indicator, bicinchoninic acid (BCA) (ε_{562} = 7700 M^{-1}).[31]

$Cu(CH_3CN)_4PF_6$ (0.1−2 equiv) in CD_3CN (47.5 mM) was added to compound **8** (1.27 mg, 0.0036 mmol) or **10** (1.5 mg, 0.0036 mmol) in DMSO-d_6 (0.6 mL), and $^1H/^{31}P$ NMR spectra were measured at 200 and 81 MHz, respectively.

■ ASSOCIATED CONTENT

Ⓢ Supporting Information

Tables of data including crystallographic and structural information; NMR spectra. This material is available free of charge via the Internet at http://pubs.acs.org.

■ AUTHOR INFORMATION

Corresponding Author

*E-mail: bilha.fischer@biu.ac.il. Fax: 972-3-6354907. Phone: 972-3-5318303.

Author Contributions

[§]These authors equally contributed to this work

Notes

The authors declare no competing financial interest.

■ ACKNOWLEDGMENTS

The authors wish to thank Dr. K. Adamsky from the Chemistry Department at BIU for her help with solid-state NMR measurements.

■ REFERENCES

(1) Jomova, K.; Valko, M. *Toxicology* **2011**, *283*, 65−87.
(2) Rooney, J. P. K. *Toxicology* **2007**, *234*, 145−156.
(3) Delangle, P.; Mintz, E. *Dalton Trans.* **2012**, *41*, 6359−6370.
(4) Amir, A.; Shmuel, E.; Zagalsky, R.; Sayer, A. H.; Nadel, Y.; Fischer, B. *Dalton Trans.* **2012**, *41*, 8539−8549.
(5) Crisponi, G.; Nurchi, V. M.; Fanni, D.; Gerosa, C.; Nemolato, S.; Faa, G. *Coord. Chem. Rev.* **2010**, *254*, 876−889.
(6) Wang, X.; Li, W.; Meng, S.; Li, D. *J. Chem. Technol. Biotechnol.* **2006**, *81*, 761−766.
(7) Amir, A.; Sayer, A. H.; Zagalsky, R.; Shimon, L. J. W.; Fischer, B. *J. Org. Chem.* **2012**, *78*, 270−277.
(8) Amir, A.; Sayer, A. H.; Ezra, A.; Fischer, B. *Inorg. Chem.* **2013**, *52*, 3133−3140.
(9) Ly, T. Q.; Woollins, J. D. *Coord. Chem. Rev.* **1998**, *176*, 451−481.
(10) Cupertino, D.; Keyte, R.; Slawin, A. M. Z.; Williams, D. J.; Woollins, J. D. *Inorg. Chem.* **1996**, *35*, 2695−2697.
(11) Maganas, D.; Grigoropoulos, A.; Staniland, S. S.; Chatziefthimiou, S. D.; Harrison, A.; Robertson, N.; Kyritsis, P.; Neese, F. *Inorg. Chem.* **2010**, *49*, 5079−5093.
(12) Bolundut, L.; Haiduc, I.; Ilyes, E.; Kociok-Kohn, G.; Molloy, K. C.; Gomez-Ruiz, S. *Inorg. Chim. Acta* **2010**, *363*, 4319−4323.
(13) Moore, P.; Errington, W.; Sangha, S. P. *Helv. Chim. Acta* **2005**, *88*, 782−795.
(14) Bereman, R. D.; Wang, F. T.; Najdzionek, J.; Braitsch, D. M. *J. Am. Chem. Soc.* **1976**, *98*, 7266−7268.
(15) Preda, A. M.; Silvestru, A.; Farcas, S.; Bienko, A.; Mrozinski, J.; Andruh, M. *Polyhedron* **2008**, *27*, 2905−2910.
(16) Silvestru, C.; Drake, J. E. *Coord. Chem. Rev.* **2001**, *223*, 117−216.
(17) Haiduc, I. *J. Organomet. Chem.* **2001**, *623*, 29−42.
(18) Aragoni, M. C.; Arca, M.; Carrea, M. B.; Demartin, F.; Devillanova, F. A.; Garau, A.; Hursthouse, M. B.; Huth, S. L.; Isaia, F.; Lippolis, V.; Ogilvie, H. R.; Verani, G. *Eur. J. Inorg. Chem.* **2006**, *2006*, 200−206.
(19) Huber, C. P.; Post, M. L.; Siiman, O. *Acta Crystallogr., Sect. B* **1978**, *34*, 2629−2632.
(20) Hong, P.; Li, C.; Banerji, S. K.; Wang, Y. *J. Hazard. Mater.* **2002**, *94*, 253−272.
(21) Magennis, S. W.; Parsons, S.; Corval, A.; Woollins, J. D.; Pikramenou, Z. *Chem. Commun.* **1999**, 61−62.
(22) Ishikawa, H.; Kido, T.; Umeda, T.; Ohyama, H. *J. Pestic. Sci.* **1992**, *56*, 1882−1883.
(23) Kumar, V.; Ahamad, T.; Nishat, N. *Eur. J. Med. Chem.* **2009**, *44*, 785−793.
(24) Morley, J. O.; Charlton, M. H. *J. Phys. Chem. A* **1998**, *102*, 6871−6876.
(25) Birdsall, D. J.; Slawin, A. M. Z.; Woollins, J. D. *Polyhedron* **2001**, *20*, 125−134.
(26) Bharara, M. S.; Parkin, S.; Atwood, D. A. *Inorg. Chem.* **2006**, *45*, 2112−2118.
(27) Britigan, B. E.; Coffman, T.; Buettner, G. *J. Biol. Chem.* **1990**, *265*, 2650−2656.
(28) Richter, Y.; Fischer, B. *J. Biol. Inorg. Chem.* **2006**, *11*, 1063−1074.
(29) Anzai, K.; Aikawa, T.; Furukawa, Y.; Matsushima, Y.; Urano, S.; Ozawa, T. *Arch. Biochem. Biophys.* **2003**, *415*, 251−256.
(30) Bohm, V.; Puspitasari-Nienaber, N. L.; Ferruzzi, M. G.; Schwartz, S. J. *J. Agric. Food Chem.* **2002**, *50*, 221−226.
(31) Brenner, A. J.; Harris, E. D. *Anal. Biochem.* **1995**, *226*, 80−84.